Assessing the Efficacy of High-Resolution Satellite-Based PERSIANN-CDR Precipitation Product in Simulating Streamflow

HAMED ASHOURI,[a] PHU NGUYEN, ANDREA THORSTENSEN, KUO-LIN HSU, SOROOSH SOROOSHIAN, AND DAN BRAITHWAITE

Center for Hydrometeorology and Remote Sensing, Department of Civil and Environmental Engineering, University of California, Irvine, Irvine, California

(Manuscript received 2 October 2015, in final form 17 May 2016)

ABSTRACT

This study aims to investigate the performance of Precipitation Estimation from Remotely Sensed Information Using Artificial Neural Networks–Climate Data Record (PERSIANN-CDR) in a rainfall–runoff modeling application over the past three decades. PERSIANN-CDR provides precipitation data at daily and 0.25° temporal and spatial resolutions from 1983 to present for the 60°S–60°N latitude band and 0°–360° longitude. The study is conducted in two phases over three test basins from the Distributed Hydrologic Model Intercomparison Project, phase 2 (DMIP2). In phase 1, a more recent period of time (2003–10) when other high-resolution satellite-based precipitation products are available is chosen. Precipitation evaluation analysis, conducted against stage IV gauge-adjusted radar data, shows that PERSIANN-CDR and TRMM Multisatellite Precipitation Analysis (TMPA) have close performances with a higher correlation coefficient for TMPA (~0.8 vs 0.75 for PERSIANN-CDR) and almost the same root-mean-square deviation (~6) for both products. TMPA and PERSIANN-CDR outperform PERSIANN, mainly because, unlike PERSIANN, TMPA and PERSIANN-CDR are gauge-adjusted precipitation products. The National Weather Service Office of Hydrologic Development Hydrology Laboratory Research Distributed Hydrologic Model (HL-RDHM) is then forced with PERSIANN, PERSIANN-CDR, TMPA, and stage IV data. Quantitative analysis using five different statistical and model efficiency measures against USGS streamflow observation show that in general in all three DMIP2 basins, the simulated hydrographs forced with PERSIANN-CDR and TMPA have close agreement. Given the promising results in the first phase, the simulation process is extended back to 1983 where only PERSIANN-CDR rainfall estimates are available. The results show that PERSIANN-CDR-derived streamflow simulations are comparable to USGS observations with correlation coefficients of ~0.67–0.73, relatively low biases (~5%–12%), and high index of agreement criterion (~0.68–0.83) between PERSIANN-CDR-simulated daily streamflow and USGS daily observations. The results prove the capability of PERSIANN-CDR in hydrological rainfall–runoff modeling application, especially for long-term streamflow simulations over the past three decades.

1. Introduction

Streamflow is one of the most important components of the hydrological cycle. Many efforts have been made to develop different models to emulate the hydrological cycle and simulate streamflow. Examples are statistical data-driven (e.g., Kim and Barros 2001; Sahoo et al. 2006; Piotrowski et al. 2006) or physically based (Estupina-Borrell et al. 2006; Sirdas and Sen 2007; Beven 2011) models in the forms of lumped [e.g., Sacramento Soil Moisture Accounting (SAC-SMA; Burnash et al. 1973) and Hydrologiska Byråns Vattenbalansavdelning (HBV; Bergstrom 1995)], semilumped [e.g., Variable Infiltration Capacity model (VIC); Liang et al. 1994], and distributed [e.g., Hydrology Laboratory Research Distributed Hydrologic Model (HL-RDHM); Koren et al. 2003, 2004, 2007]. One of the most, if not the most, important criteria in all of these types of hydrological modeling schemes, but particularly in the distributed format, is the availability of high-quality data with desirable spatial and

[a] Current affiliation: AIR Worldwide, Boston, Massachusetts.

Corresponding author address: Hamed Ashouri, Center for Hydrometeorology and Remote Sensing, Department of Civil and Environmental Engineering, University of California, Irvine, E/4130 Engineering Gateway, Irvine, CA 92617.
E-mail: h.ashouri@uci.edu

DOI: 10.1175/JHM-D-15-0192.1

temporal coverages. Satellite products with their global coverage are very well suited for this purpose. With the advancement in remote sensing science and technology, high-resolution data and information about the earth's surface characteristics (e.g., topography, soil types, and land use) and hydrometeorological forcings (e.g., precipitation, temperature, and evapotranspiration) have been made available globally. Particularly, remote sensing of precipitation—one of the key hydrometeorological variables in generating floods—has gained significant attention in the recent past. Numerous efforts have been made to produce satellite-based precipitation estimates at high spatiotemporal resolution in global scale. Examples are the CPC morphing technique (CMORPH; Joyce et al. 2004), Precipitation Estimation from Remotely Sensed Information Using Artificial Neural Networks (PERSIANN; Hsu et al. 1997, 1999; Sorooshian et al. 2000), PERSIANN–Climate Data Record (PERSIANN-CDR; Ashouri et al. 2015), Tropical Rainfall Measuring Mission (TRMM) Multisatellite Precipitation Analysis (TMPA; Huffman et al. 2007), the Naval Research Laboratory (NRL)-Blend satellite rainfall estimates (Turk et al. 2010), and the Integrated Multisatellite Retrievals for Global Precipitation Measurement (IMERG; Huffman et al. 2015). Such products are valuable sources of information and data for flood modeling in a distributed format.

Previous efforts have been made in evaluating the accuracy of different satellite-based precipitation products against gauge observations (e.g., Sorooshian et al. 2000; Hong et al. 2006; Ebert et al. 2007; Miao et al. 2015; Ashouri et al. 2016) and utilizing such data in different applications, especially hydrological modeling (see Behrangi et al. 2011; Bajracharya et al. 2015; Maggioni et al. 2013; Nguyen et al. 2014, 2015, 2016; Seyyedi et al. 2015). Feasibility of using satellite-based precipitation as input for hydrologic simulation has been demonstrated in the Mediterranean (Ciabatta et al. 2016) and for simulating high flows in Africa (Thiemig et al. 2013). However, certain challenges and limitations with using satellite-based precipitation for rainfall–runoff modeling have been identified. Of reoccurring concern is bias in satellite-based precipitation estimates that carries over to hydrological simulations when used as model input (Guetter et al. 1996; Stisen and Sandholt 2010; Thiemig et al. 2013). Harris et al. (2007) also point to spatial resolution of coarse satellite-based precipitation products as a concern for use in hydrologic models, cautioning their use in an operational setting, and recommending adjustments to the precipitation estimates even beyond simple bias adjustments.

In this study, we implement a newly developed precipitation climate data record, PERSIANN-CDR, into a long-term hydrological modeling framework to simulate historical streamflow and flood events. In other words, we seek to evaluate the performance of PERSIANN-CDR in a distributed rainfall–runoff modeling application and compare its performance with other high-resolution precipitation products. For this purpose, the National Weather Service (NWS) HL-RDHM is used. This study is conducted in two phases. In the first phase, a period of time when PERSIANN-CDR, TMPA, and stage IV gauge-adjusted radar data products are available is chosen and the hydrological modeling is performed for this period. The study period for this phase is selected from 2003 to 2010 when all the aforementioned precipitation products are available. The results of this phase reveal how PERSIANN-CDR performs compared with the well-established TMPA data product as far as generating streamflow in the study basin. In the second phase, the entire record of the 0.25° daily PERSIANN-CDR data is used to extend the modeling process back to 1983, allowing for long-term streamflow simulations conducted at a higher resolution than previously possible.

The paper is structured as follows: section 2 describes the data used in this study, section 3 provides detailed information about the methodology and modeling structure, section 4 presents the results, and section 5 concludes with a summary of the main findings.

2. Data

a. TMPA

TRMM, a joint mission between NASA and the Japan Aerospace Exploration Agency (JAXA), was launched in November 1997 with a design lifetime of 3 years. TRMM, however, produced more than 17 years of data to study tropical rainfall for weather and climate research. This mission officially came to an end on 15 April 2015. As one of the TRMM products, TMPA (Huffman et al. 2007, 2010) contains near-global (50°S–50°N) precipitation data at 3-hourly temporal resolution and 0.25° × 0.25° grid cells. In this study, version 7 of this product is used. TMPA has an established record in precipitation and hydrological modeling studies (for a complete list of TMPA citations, refer to ftp://precip.gsfc.nasa.gov/pub/trmmdocs/rt/TMPA_citations.pdf). From the hydrological modeling perspective, Su et al. (2008) forced the VIC with TMPA precipitation data over La Plata basin in South America. The study reported that the TMPA-driven simulations were able to capture the daily flooding events and to represent low flows, although upward biases were identified in peak flows. Another study

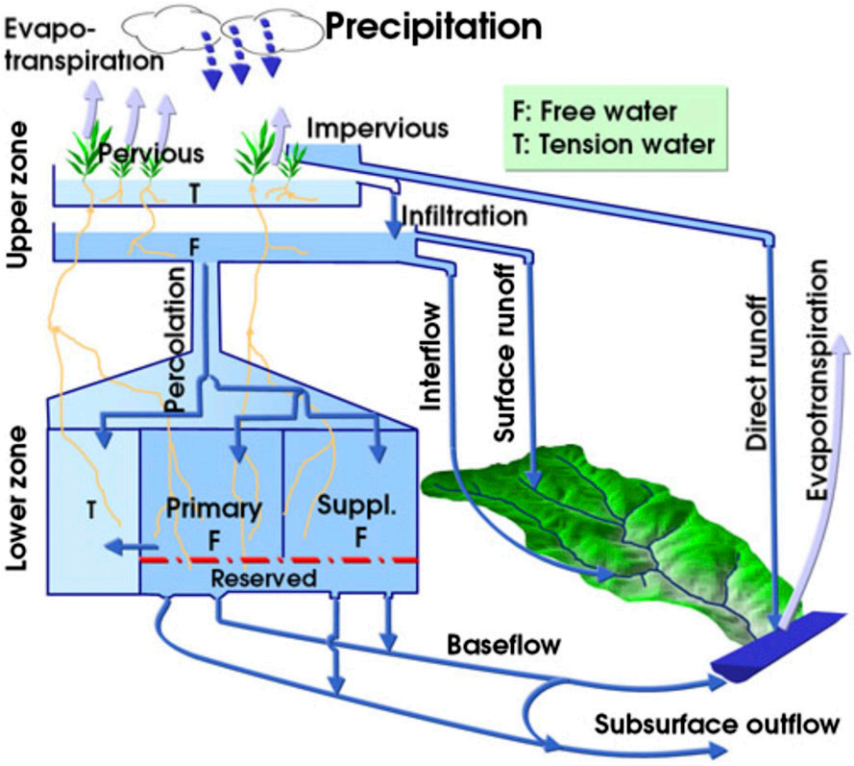

FIG. 1. Schematic of the SAC-SMA (Burnash et al. 1973; image source: http://ldas.gsfc.nasa.gov/nldas/images/SAC_schematic.jpg).

over the Amazon basin (Collischonn et al. 2008) showed that the TRMM-based simulated hydrographs depicted comparable performance to those calculated from rain gauge data. Given the findings of such studies, in order to compare the performance of PERSIANN-CDR with another high-resolution satellite-based precipitation product, TMPA 3B42, version 7 (hereafter TMPA), for the period of 2003–10 is chosen.

b. *PERSIANN-CDR*

PERSIANN-CDR (Ashouri et al. 2015) is a newly developed and released satellite-based precipitation product that covers more than three decades (from 1 January 1983 to present) of daily precipitation estimations at 0.25° resolution for the 60°S–60°N latitude band. PERSIANN-CDR uses the archive of infrared brightness temperature CDR from Gridded Satellite (GridSat)-B1 (Knapp 2008a,b; Knapp et al. 2011) in the International Satellite Cloud Climatology Project (ISCCP; Rossow and Schiffer 1991; Rossow and Garder 1993) as the input to the trained neural network of the PERSIANN model. The resulting rainfall estimates are then corrected for bias using the monthly Global Precipitation Climatology Project (GPCP), version 2.2, 2.5° product. The dataset has been released and made available for public access through NOAA/National Centers for Environmental Information (NCEI; http://www1.ncdc.noaa.gov/pub/data/sds/cdr/CDRs/PERSIANN/Overview.pdf). PERSIANN-CDR has already shown its usefulness for a relatively wide range of different applications (Guo et al. 2015; Solmon et al. 2015; Ceccherini et al. 2015; Yong 2015; Yang et al. 2016). Using different extreme precipitation indices, Miao et al. (2015) evaluated the performance of PERSIANN-CDR in capturing the behavior of historical extreme precipitation events over China. Their results showed the capability of PERSIANN-CDR in reproducing similar spatial and temporal patterns of daily precipitation extremes as those depicted by the East Asia (EA) ground-based gridded daily precipitation dataset. In another study by Hagos et al. (2016) that investigated changes in the frequency of landfalling atmospheric river and extreme precipitation in the simulation of the Community Earth System Model (CESM), PERSIANN-CDR was used as the ''observation'' precipitation. Luchetti et al. (2016) used PERSIANN-CDR in a NOAA–NASA collaborative project for updating the ENSO-based rainfall climatology for regions in Hawaii and U.S.-affiliated Pacific islands. With respect to the applicability of PERSIANN-CDR, the paper concludes that their results ''solidified the

TABLE 1. HL-RDHM parameter descriptions and their basin-average values (Koren et al. 2004).

Parameter	Description	SLOA4	ELMSP	SAVOY
SAC-HT				
sac_UZTWM (mm)	Upper-zone tension water capacity	68.46	74.74	51.41
sac_UZFWM (mm)	Upper-zone free water capacity	20.52	21.17	18.11
sac_UZK (day^{-1})	Fractional daily upper-zone free	0.2978	0.2775	0.3427
sac_ZPERC (DL)	Max percolation rate	117.9	125.9	100.5
sac_REXP (DL)	Exponent for the percolation equation	2.026	2.065	1.943
sac_LZTWM (mm)	Lower-zone tension water capacity			
sac_LZFSM (mm)	Lower-zone supplemental free water capacity	173	177.1	163.2
sac_LZFPM (mm)	Lower-zone primary free water capacity	83.57	74.87	101.6
sac_LZSK (day^{-1})	Fractional daily supplemental withdrawal rate	0.1140	0.1074	0.1285
sac_LZPK (day^{-1})	Fractional daily primary withdrawal rate	0.017 04	0.017 54	0.015 13
sac_PFREE	Percolation fraction that always goes directly to lower-zone free water storages	0.3591	0.3743	0.3304
Rutpix9				
rutpix_Q0CHN	Specific channel discharge per unit channel cross-sectional area	0.3281	0.3389	0.3377
rutpix_QMCHN (DL)	Power value in relationship between discharge and cross section	1.288	1.288	1.288
sac_PCTIM (fraction)	Min impervious area	0.001	0.001	0.001
sac_ADIMP (fraction)	Additional impervious area	0	0	0
sac_RIVA (fraction)	Riparian vegetation area	0.035	0.035	0.035
sac_SIDE (fraction)	Ratio of nonchannel base flow to channel base flow	0	0	0
sac_RSERV	Lower-zone free water fraction that cannot be transferred to lower-zone tension water	0.3	0.3	0.3
sac_EFC (fraction)	Effective forest cover	0	0	0

ability of the high resolution PERSIANN-CDR to be more than adequate for use in long-term precipitation climatology studies.'' With respect to hydrological application, Casse and Gosset (2015) used PERSIANN-CDR to study hydrological changes and flood increases in the Niger River and the city of Niamey (Niger) over the period of 1983–2013. The results showed that PERSIANN-CDR produces annual rainfall amounts comparable with those from gauge-adjusted satellite rainfall estimates and gauge data. The paper also concludes that ''the PERSIANN-CDR based hydrological simulation presents a realistic inter-annual variability, and detects flooded years, but not the exact flooded period day by day'' (Casse and Gosset 2015, p. 122).

c. *Stage IV gauge-adjusted radar data*

National Centers for Environmental Prediction (NCEP) Environmental Modeling Center (EMC) provides the stage IV gauge-adjusted precipitation product (Fulton et al. 1998) from high-resolution Doppler Next Generation Weather Radar (NEXRAD) network and hourly rain gauge data over the contiguous United States. Stage IV radar data are available at 1-, 6-, and 24-hourly scales at 4-km spatial resolution at Hydrologic Rainfall Analysis Project (HRAP) national grid system. Stage IV radar data are manually quality controlled at NWS River Forecast Centers (RFCs). (More information about stage IV data can be obtained from www.emc.ncep.noaa.gov/mmb/ylin/pcpanl/stage4/.) Stage IV precipitation data have been used in different studies (e.g., Ebert et al. 2007; Zeweldi and Gebremichael 2009; Anagnostou et al. 2010; Ashouri et al. 2015). In this study, stage IV data are first used as the reference data for evaluating satellite-based precipitation products. They are then used as a forcing data into the hydrological model to generate streamflow simulations.

In this study, all data products are first scaled to 0.25° and daily spatiotemporal resolution before use.

3. Methodology

As introduced earlier, the main goal of this study is to investigate the performance of the newly developed precipitation climate data record, PERSIANN-CDR, in a hydrological rainfall–runoff modeling application and compare its performance with other precipitation products. For this purpose, the NOAA/NWS/Office of Hydrologic Development's HL-RDHM (Koren et al. 2003, 2004, 2007) is used as the hydrological model to simulate the streamflow using the precipitation data products. HL-RDHM has been widely used for hydrologic studies (e.g., Smith et al. 2004; Reed et al. 2007; Tang et al. 2007; Yilmaz et al. 2008; Wagener et al. 2009; Khakbaz et al. 2012; Smith et al. 2012a,b). The conceptually based SAC-SMA provides the foundation of HL-RDHM. A schematic of SAC-SMA is shown in Fig. 1. SAC-SMA features two conceptual layers, upper- and lower-zone storage, both of which have two basic components, tension water and free

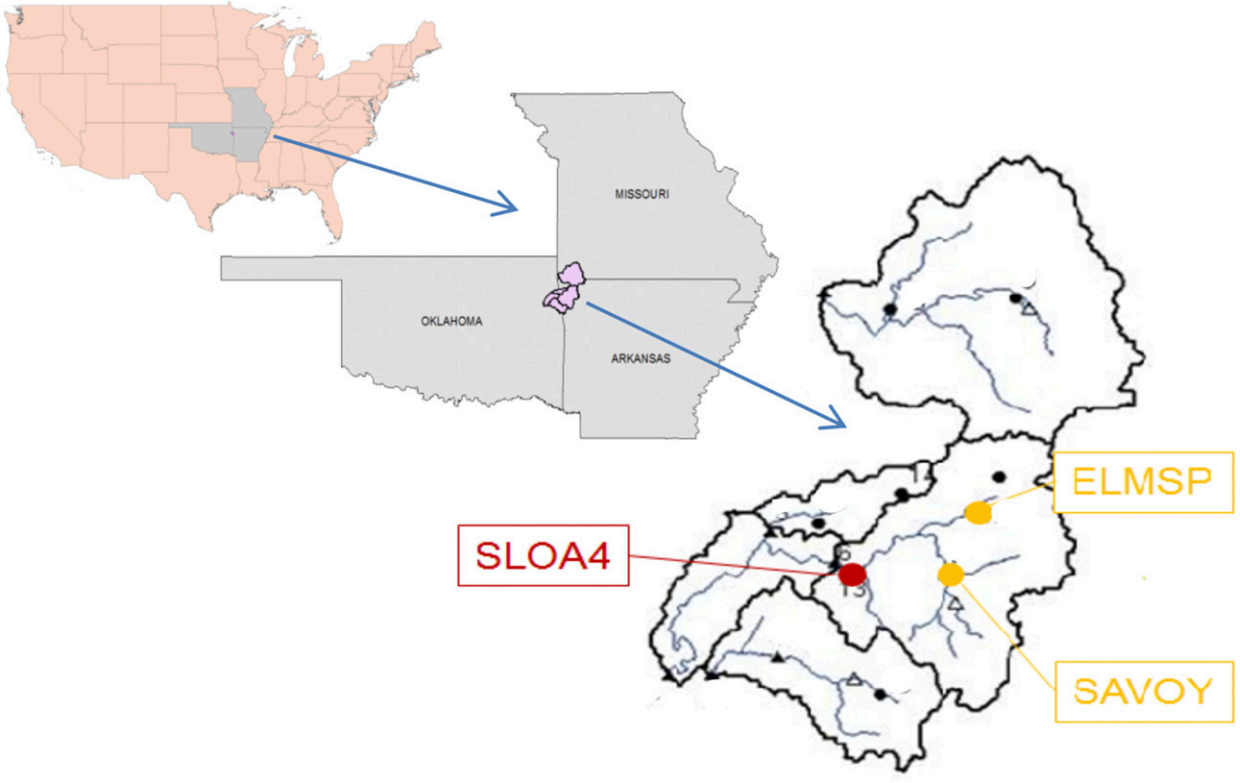

FIG. 2. The three study basins (SAVOY, ELMSP, and SLOA4) [modified from Smith et al. (2012)].

water. An enhanced version of SAC-SMA known as the Sacramento Soil Moisture Accounting Heat Transfer (SAC-HT) includes the use of Noah land surface model–based physics to estimate a physically meaningful soil moisture profile, allowing for the estimation of heat transfer within the column (Koren et al. 2007). The second HL-RDHM module that this study uses is a routing scheme known as Rutpix9. This scheme consists of a hillslope component in which fast (overland flow) runoff is routed over a uniform conceptual hillslope and is combined with a slow (subsurface flow) component. Following hillslope runoff generation, a channel-routing process moves water downstream using a topographically based, cell-to-cell method. In Rutpix9, the relationship between discharge and channel cross section is based on the rating curve method (NWS 2011).

With respect to the calibration of the hydrological model, many studies have made a case for input-specific model calibration in order to compensate for possible pitfalls associated with a specific satellite precipitation product (e.g., Ciabatta et al. 2016; Qi et al. 2016; Stisen and Sandholt 2010; Thiemig et al. 2013). While this technique allows for multiple satellite products to yield satisfactory hydrologic simulation performance despite discrepancies in precipitation estimates, it hinders efforts to improve the precipitation product as well as the model by allowing the two to compensate for one another's deficiencies. For this reason, the work presented here relies on calibration of the model by experts who used precipitation estimates they deemed as the most dependable (based on radar in this case) for the particular model/study region. These parameters are held constant for evaluation across all precipitation products rather than performing product-specific calibration. This allows us to focus our evaluation solely on the performance of the precipitation products without their performance being altered by the potential improvements that product-specific calibration would bring. For HL-RDHM, the model has been expertly calibrated by the NWS for the Distributed Hydrologic Model Intercomparison Project, phase 2 (DMIP2), basins. A priori parameter sets have been derived from soil and land-use data for HL-RDHM. Scalar multipliers of these parameter sets are used for calibration, assuming that the relationship of the individual pixels to one another is adequately characterized in the a priori sets. In this study, we rely on these expertly calibrated parameters by NWS experts for the calibration of the hydrological model. The calibrated parameters for SAC-HT and Rutpix9 provided by NWS are summarized as

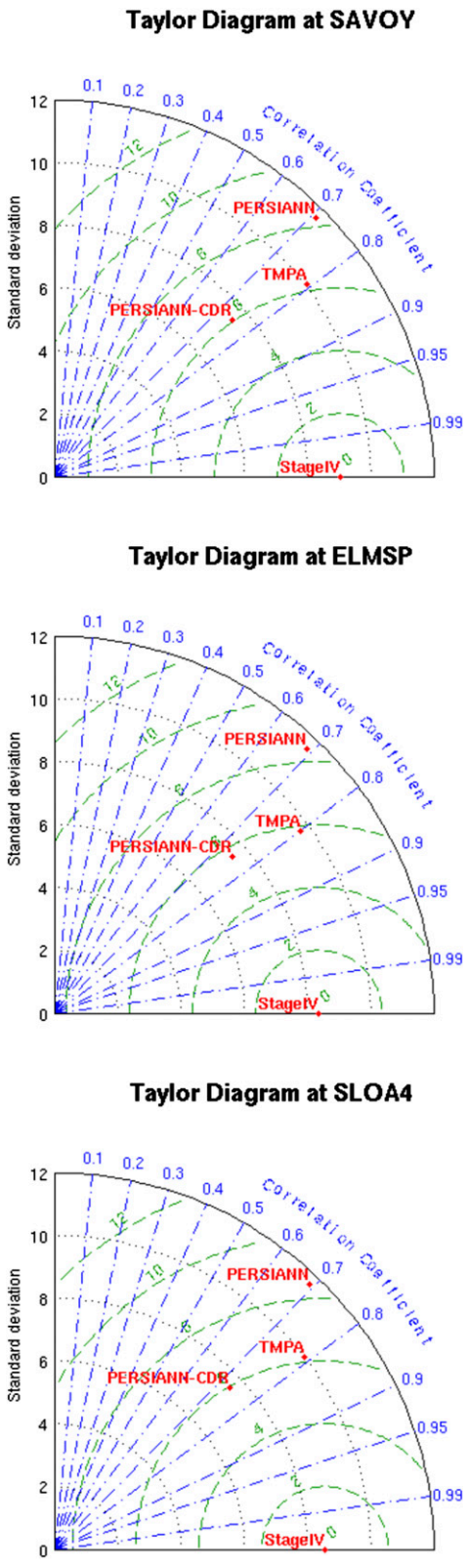

FIG. 3. Precipitation comparison plots for (top) SAVOY, (middle) ELMSP, and (bottom) SLOA4 basins for 2003–10.

basin-average values in Table 1. Detailed information about HL-RDHM can be found in its user manual (NWS 2011; Koren and Barrett 1994).

With respect to the study area, three basins from the Oklahoma test basins from DMIP2 are chosen (Fig. 2). The two smaller study basins with outlets at Osage Creek near Elm Springs, Arkansas (ELMSP), and the Illinois River at Savoy, Arkansas (SAVOY), have drainage areas of 337 and 433 km^2 and feed into the third study basin, which has an outlet located on the Illinois River south of Siloam Springs, Arkansas (SLOA4), and a drainage area of 1489 km^2 (Smith et al. 2012). The Illinois River basin encompasses the three study basins and is characterized by an annual rainfall of ~1200 mm (Smith et al. 2004). It is noteworthy that the selection of these three test basins is based on the availability of the a priori calibrated parameter sets from NWS, which were only available for these three basins at the time of this study.

Prior to setting up the hydrological modeling scheme, a preliminary evaluation on the accuracy of the utilized precipitation products against stage IV gauge-adjusted radar data is conducted. After having the model structure in place, HL-RDHM is run in two phases. In the first phase, the time period of 2003–10 when all products (PERSIANN, PERSIANN-CDR, TMPA, and stage IV) are available is selected. The resulting hydrographs from HL-RDHM forced with the three precipitation products at the three study basins are compared with the USGS streamflow observations. The results of this phase depict how PERSIANN-CDR-simulated streamflow compares with other currently available precipitation products, that is, TMPA and stage IV data. Having proven the concept, in the second phase we extend the simulation process back to 1983, where only PERSIANN-CDR data are available.

To assess the closeness of the simulated streamflow to the USGS observations, the following statistical measures are calculated. In addition to correlation coefficient (CORR), centered root-mean-square error (RMSE), and percent volume bias (BIAS), the Nash–Sutcliffe coefficient E and index of agreement d is investigated. The Nash–Sutcliffe coefficient (Nash and Sutcliffe 1970) is an efficiency criterion that is calculated as 1 minus the sum of the squared differences between observed and simulated values normalized by the variance of the observations:

$$E = 1 - \frac{\sum_{i=1}^{N} (\mathrm{Obs}_i - \mathrm{Sim}_i)^2}{\sum_{i=1}^{N} (\mathrm{Obs}_i - \overline{\mathrm{Obs}})^2},$$

where Obs_i and Sim_i are the observed and simulated values at time step i, respectively; $\overline{\mathrm{Obs}}$ is the mean of the observation; and E ranges from $-\infty$ to 1, with 1 being the

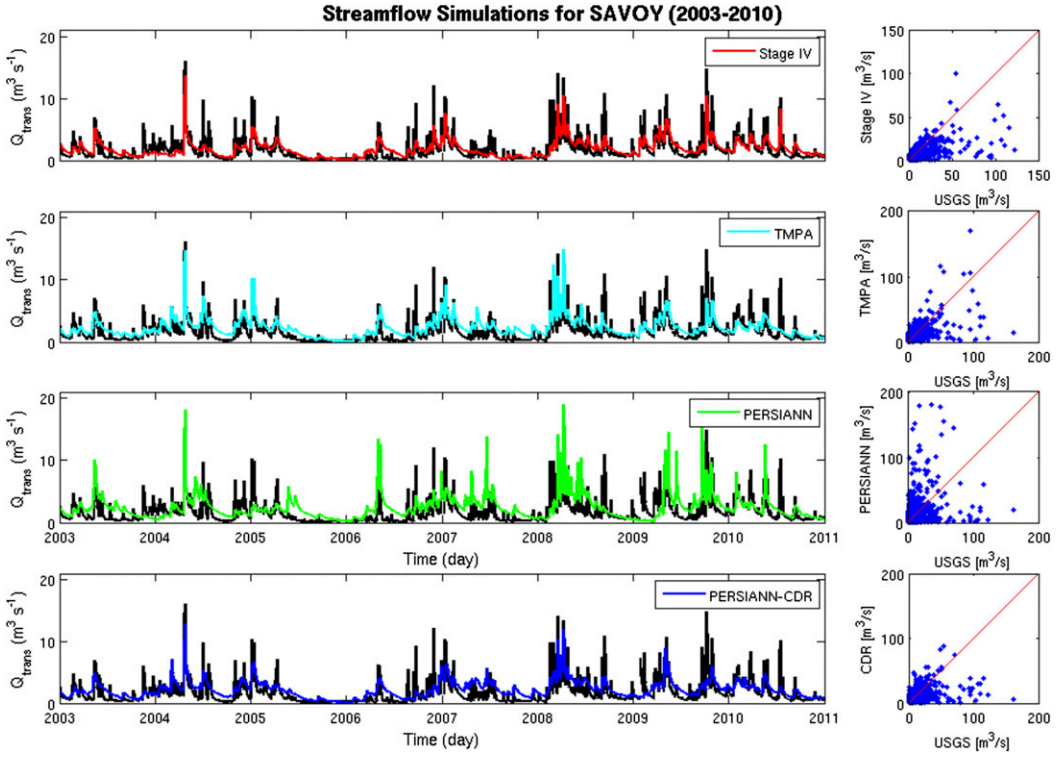

FIG. 4. Simulated and observed streamflow hydrographs and respective scatterplots at the outlet of SAVOY basin using (from top to bottom) stage IV, TMPA, PERSIANN, and PERSIANN-CDR precipitation products. The solid black line shows the USGS observations.

perfect fit and negative values indicating that the mean of the observation would be a better predictor than the model. The main drawback of the Nash–Sutcliffe criterion is that, since the differences are squared, this efficiency criterion is biased toward peak values and less sensitive during low-flow periods (Legates and McCabe 1999). To overcome this problem, E is often calculated based on the logarithmic values of the observed and simulated data. In this study, we take the ln E approach.

The index of agreement (Willmot 1984) is calculated as 1 minus the squared differences between the observed and simulated values normalized by the largest potential error. The variable d is calculated using the following equation and ranges from 0 to 1, with 1 being the perfect fit:

$$d = 1 - \frac{\sum_{i=1}^{N} (\mathrm{Obs}_i - \mathrm{Sim}_i)^2}{\sum_{i=1}^{N} (|\mathrm{Sim}_i - \overline{\mathrm{Obs}}| + |\mathrm{Obs}_i - \overline{\mathrm{Obs}}|)^2}.$$

The results of the two phases of the study are provided in the section below.

4. Results

Before conducting the hydrological modeling process, it is necessary to evaluate the accuracy of the precipitation products over the study region. A comparison of PERSIANN, PERSIANN-CDR, and TMPA precipitation products against stage IV gauge-adjusted radar data as our reference dataset is conducted. Basic precipitation evaluation statistics, including correlation coefficient, standard deviation, and root-mean-square deviation, are presented on Taylor diagrams (Fig. 3). The results show that, in the three study basins, TMPA and PERSIANN-CDR have close performances, with slightly higher correlation coefficient for TMPA (~0.8 vs 0.75 for PERSIANN-CDR) and similar RMSD (~6 mm day^{-1}) for both products. TMPA shows a higher standard deviation (~10 mm day^{-1}) than PERSIANN-CDR (~8 mm day^{-1}). TMPA and PERSIANN-CDR both outperform PERSIANN, mainly because, unlike PERSIANN, TMPA and PERSIANN-CDR are gauge-adjusted precipitation products.

Given the results of the previous section showing a reasonably accurate performance of PERSIANN-CDR and TMPA when compared to stage IV radar data, we

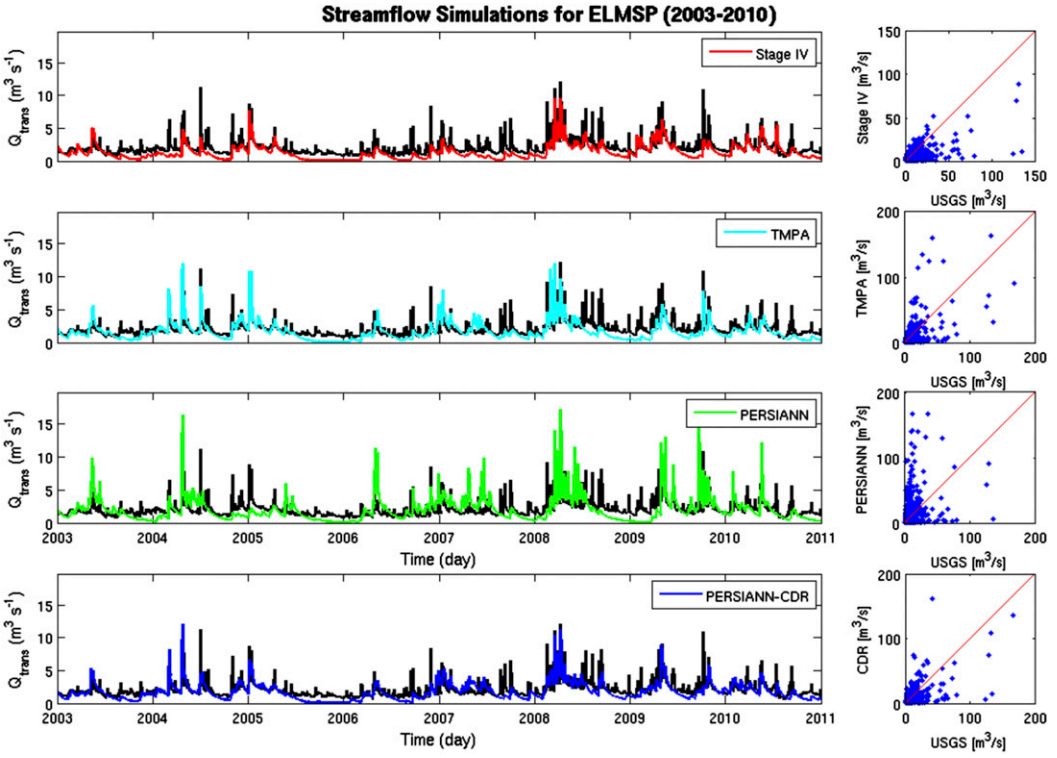

FIG. 5. As in Fig. 4, but for ELMSP basin.

can reliably use these precipitation datasets as the forcing to the hydrological model. In the first phase, the simulation process is performed for 2003–10 when all four precipitation products are available. As mentioned in the methodology section, the HL-RDHM is used as our hydrological model. With respect to calibration, we relied on the calibrated a priori parameter set (see Table 1), by NWS experts, for the basins we used. After setting up the model, HL-RDHM is forced with the PERSIANN, PERSIANN-CDR, TMPA, and stage IV precipitation products to simulate streamflow Q at the outlet of the three study basins. The USGS streamflow observations are used as the reference streamflow data. For a better visualization of the resulted hydrographs, especially for peak and low flows, we used the following transformation function proposed by Hogue et al. (2000) and used in different studies (Yilmaz et al. 2005; Khakbaz et al. 2012; Behrangi et al. 2011):

$$Q_{\text{trans}} = \frac{(Q+1)^{0.3} - 1}{0.3}.$$

The resulting streamflow simulations Q_{trans} for SAVOY, ELMSP, and SLOA4 basins are shown in Figs. 4–6, respectively. The scatterplots of nontransformed flows against the USGS observations (black line) are shown in Figs. 4–6 (right). In general, for all three DMIP2 basins stage IV radar data seem to outperform the other products. The simulated hydrograph results from PERSIANN-CDR and TMPA forcing generally show close agreement. For quantitative comparisons, different statistical measures including CORR, RMSE, BIAS, ln E, and d are calculated from the PERSIANN-, PERSIANN-CDR-, TMPA-, and stage IV–derived hydrographs when compared with USGS observations. As shown in the Taylor diagrams in Fig. 7, stage IV generally outperforms other products, with higher CORR (~0.75–0.8) and lower RMSE and standard deviation in all three basins. TMPA and PERSIANN-CDR both perform well, with a higher CORR for TMPA at SAVOY and SLOA4 and a higher CORR for PERSIANN-CDR at ELMSP basin. PERSIANN-CDR shows lower standard deviation than TMPA in all three basins. PERSIANN shows a CORR of about 0.5–0.6. The high values of RMSE for PERSIANN are due to the nature of this being a real-time product with no gauge correction. Table 2 summarizes all the statistics for the three study basins. The lower BIAS in PERSIANN-CDR compared to PERSIANN shows the effectiveness of the bias-removal algorithm in reducing the bias in satellite estimates when compared to ground measurements. Possible reasons for large bias in the stage IV radar data are given in the discussion section.

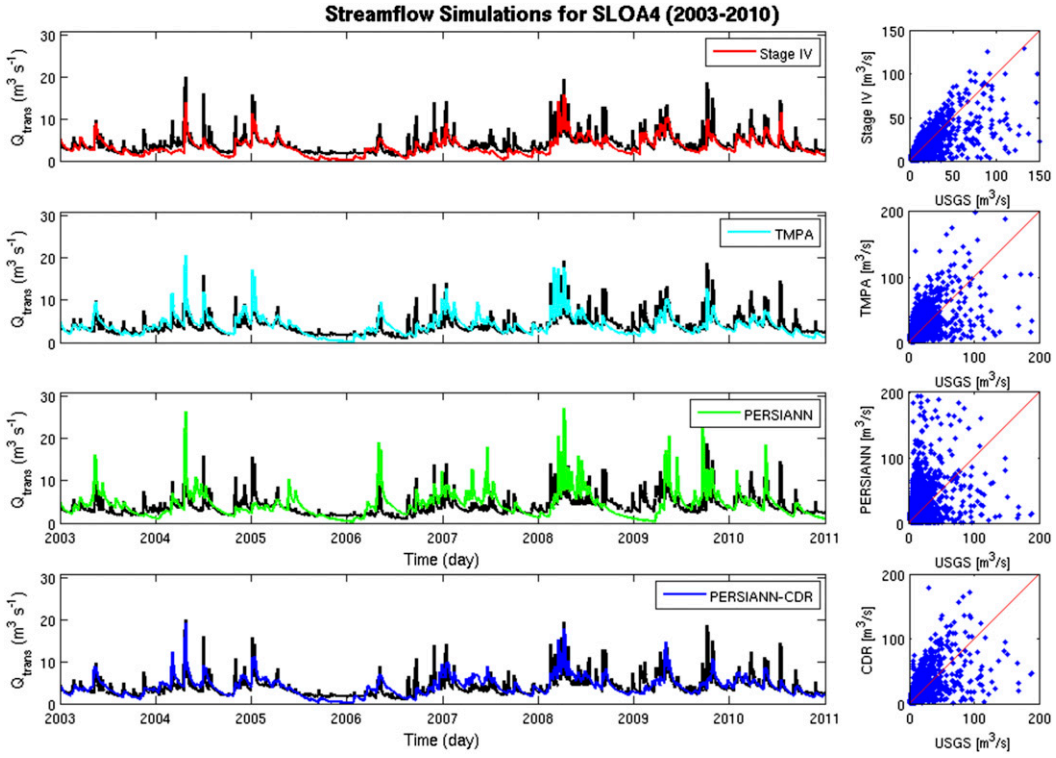

FIG. 6. As in Fig. 4, but for SLOA4 basin.

In addition to the quantitative analysis over the entire record, an analysis on the long-term (2003–10) annual cycle from daily USGS streamflow observation, as well as the stage IV–, TMPA-, PERSIANN-, and PERSIANN-CDR-derived hydrographs for the three study basins, is conducted. As shown in Fig. 8, PERSIANN-CDR and TMPA depict a relatively similar performance for all seasons. PERSIANN's performance degrades in the spring season. The improvements from PERSIANN to PERSIANN-CDR are also evident in Fig. 8. Respective daily based statistical measures from day-of-year long-term (2003–10) annual cycle analyses are calculated against gauge observations and shown in Table 3. The reduction in the percentage volume bias from PERSIANN to PERSIANN-CDR is evident. At the SAVOY basin, TMPA shows the highest index of agreement, where this measure is the highest for PERSIANN-CDR. Stage IV shows the lowest RMSE in all the three catchments. PERSIANN-CDR shows a higher RMSE than TMPA at SAVOY but a lower RMSE at ELMSP basin. RMSEs from PERSIANN-CDR and TMPA are very close at the SLOA4 basin. With respect to the CORR, stage IV radar data show the best performance at SAVOY and ELMSP basins. PERSIANN-CDR shows a slightly higher CORR than TMPA at the ELMSP basin, but TMPA outperforms PERSIANN-CDR in the SAVOY and SLOA4 basins in this regard. The large negative bias in stage IV radar data in ELMSP and SLOA4 is again observed in this analysis. The seasonal analysis (figures not presented) shows that the largest negative bias in stage IV–derived streamflow happens in the summer and fall seasons.

Results of phase 1 analyses for the period when other high-resolution, satellite-derived precipitation products are available show that the performance of PERSIANN-CDR has been close to other precipitation products. The findings of this phase reveal the high potential for PERSIANN-CDR data use in rainfall–runoff modeling applications, particularly long-term simulations of more than three decades, given the fact that PERSIANN-CDR rainfall data spans from 1 January 1983 to present (delayed) time. Therefore, in phase 2, HL-RDHM is forced with daily PERSIANN-CDR rainfall estimation for 1983–2012 to reconstruct historical streamflow at the three study basins. It is important to note that, similar to phase 1, we rely on the NWS a priori parameter sets for the calibration of the model. The resulting hydrographs for SAVOY, ELMSP, and SLOA4 are shown in Fig. 9, with the black line being the USGS observation and the blue line being the PERSIANN-CDR-derived hydrograph. As shown, an

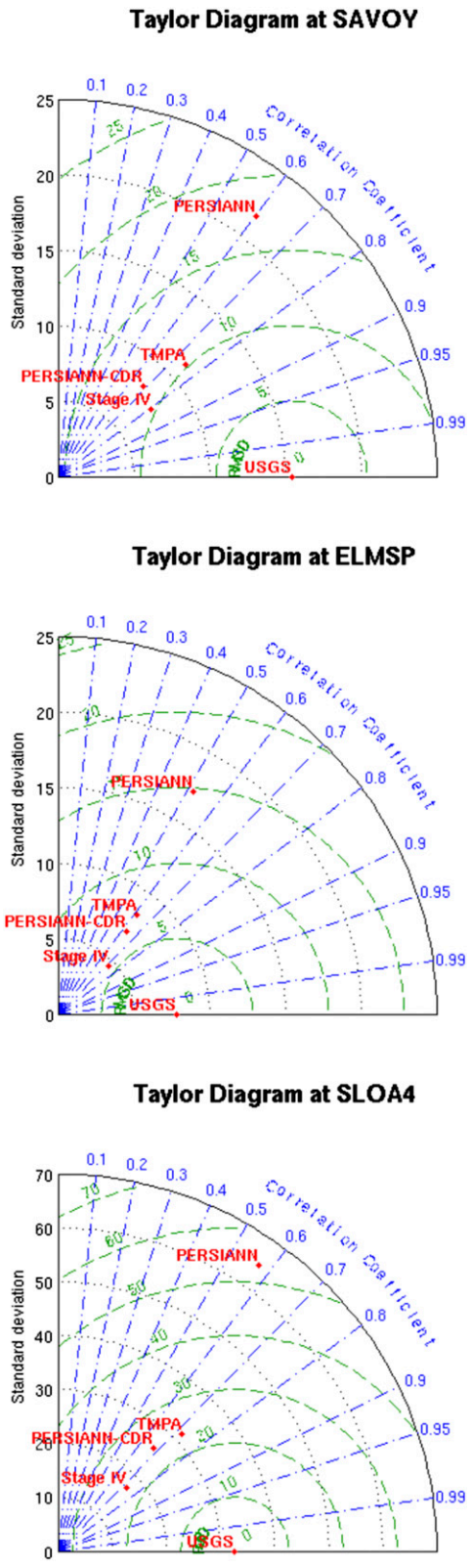

FIG. 7. Taylor diagram showing the correlation coefficient, standard deviation, and root-mean-square deviation from the PERSIANN-, PERSIANN-CDR-, TMPA-, and stage IV–derived hydrographs for (top) SAVOY, (middle) ELMSP, and (bottom) SLOA4 basins for 2003–10.

immediate result is that PERSIANN-CDR could reconstruct the full record of historical streamflow, especially for years prior to 1996 (except 1986 for SAVOY basin) when generally the USGS streamflow observations are not available for the three study basins. The scatterplots comparing the PERSIANN-CDR-simulated streamflow against USGS observations for 1983–2012 for the three study basins are shown in Fig. 9. The summary of quantitative comparisons is presented in Table 4. The results depict high CORR (~0.67–0.73), relatively low BIAS (~5%–12%), and high index of agreement criterion (~0.68–0.83) between PERSIANN-CDR-simulated daily streamflow and USGS daily observations, demonstrating reasonable performance of PERSIANN-CDR despite the calibration of the hydrological model by a precipitation product other than PERSIANN-CDR. It is also noteworthy that the efficiency index of the logarithmic Nash–Sutcliffe coefficient derived in the second phase of the study is comparable, and even slightly better, than the same coefficient in the first phase of the study for other precipitation products.

5. Discussion

There are few points what we would like to clarify via the explanations below. First, we would like to point out that the main reason for including the real-time PERSIANN product in our analysis was to investigate the progress that the Center for Hydrometeorology and Remote Sensing at the University of California, Irvine, has made over time in improving its precipitation products. Regarding this, the improvements are evident from both the precipitation and simulated streamflow points of view. That said, there are certain facts that should be considered here since a blind comparison of real-time precipitation products [e.g., PERSIANN or TMPA–real time (3B42RT)] with gauge-adjusted products (e.g., TMPA and PERSIANN-CDR) may not be a fair comparison in general. In the case of PERSIANN and PERSIANN-CDR, the latter is indirectly gauge corrected based on the gauge information from the Global Precipitation Climatology Centre (GPCC; Schneider et al. 2008) used in the GPCP monthly precipitation product (see Huffman and Bolvin 2013), whereas PERSIANN is a real-time product without any gauge-adjusting component. Real-time PERSIANN data are useful for real-time applications such as global flood monitoring, while the long-term (+30 years), daily PERSIANN-CDR rainfall data make it useful for long-term hydrological and climatological studies and applications. As is the case with other satellite-based products, the choice of PERSIANN or PERSIANN-CDR depends on the type

TABLE 2. Mean, standard deviation (std dev), centered RMSE, CORR, ln E, BIAS, and d for simulated streamflow (2003–10) from PERSIANN, PERSIANN-CDR, stage IV, and TMPA compared to USGS streamflow observations.

Product	Mean ($m^3 s^{-1}$)	Std dev ($m^3 s^{-1}$)	RMSE ($m^3 s^{-1}$)	CORR	ln E	BIAS	d
SAVOY							
PERSIANN	7.79	21.69	17.44	0.604	−0.203	61.2%	0.725
PERSIANN-CDR	5.54	8.17	11.46	0.686	0.274	14.6%	0.728
Stage IV	4.2	7.58	10.3	0.808	0.536	−13.0%	0.781
TMPA	5.86	11.2	10.2	0.750	0.254	21.2%	0.833
ELMSP							
PERSIANN	5.83	17.15	14.73	0.52	−2.47	26.6%	0.567
PERSIANN-CDR	4.14	7.1	6.36	0.648	−1.88	−10.1%	0.781
Stage IV	2.72	4.56	5.54	0.721	−4.72	−41.05%	0.756
TMPA	3.83	8.37	7.07	0.622	−2.19	−16.84%	0.767
SLOA4							
PERSIANN	25.45	64.68	53.24	0.572	−0.662	55.1%	0.631
PERSIANN-CDR	18.04	26.05	24.35	0.677	0.166	9.91%	0.798
Stage IV	12.1	17.16	23.2	0.733	−0.113	−26.34%	0.75
TMPA	17.74	31.33	23.8	0.724	0.156	8.08%	0.841

of application, period of the study, and the constraints of the problem.

The second point refers to the relatively high percent bias observed in the stage IV streamflow simulations for ELMSP and SLOA4 basins compared to PERSIANN-CDR and TMPA. There could be a couple of reasons for that. First, the validation period in this study is not the same as the calibration period for which the a priori parameters are estimated, so there is no guarantee that stage IV is always better than the other products in the discharge simulations. More importantly, calibration performed by the NWS (see Kuzmin et al. 2008) is based on a multi-time-scale form of RMSE and does not include bias in the objective function. In Table 2, stage IV simulation has the lowest RMSE that is consistent with the calibration methods. It is noteworthy that the correlations of stage IV simulations in all cases are better than the others.

The third point is about the low Nash–Sutcliff efficiency values obtained from the simulated streamflow time series. The key point here is the calibration of the hydrological model. As explained in the introduction and methodology sections, instead of conducting product-specific calibration, we relied on the NWS expertly calibrated a priori parameter sets for the calibration of the HL-RDHM for the study basins. These parameters are kept fixed for all the precipitation products, allowing us to focus our evaluation solely on the performance of the precipitation products, rather than mixing it with the improvements that product-specific calibrations of the hydrological model can, and do, introduce in the final simulations. It is obvious that by conducting product-specific calibration, one would achieve higher-efficiency results.

The fourth point is about the performance of PERSIANN-CDR in reproducing the observed peak flows during the 1983–2012 period (Fig. 9), when observations are available. Part of the mismatch is due to the fact that our hydrological model was not specifically calibrated with PERSIANN-CDR data. In addition to that, it could be partly due to the fault of the forcing precipitation, the fault of the model, or even the fault of the precipitation product used for calibration (or a combination of all).

6. Conclusions

The main goal of this study was to evaluate the performance of the newly developed precipitation climate data record, PERSIANN-CDR, in a rainfall–runoff modeling scheme and compare its performance with other high-resolution precipitation products. In examining the accuracy of the precipitation products, PERSIANN-CDR and TMPA showed close performances compared to the stage IV gauge-adjusted radar data product. Focusing only on the PERSIANN products, it is found that PERSIANN-CDR outperforms the PERSIANN real-time product, depicting better statistical measures. This is mainly because PERSIANN-CDR is gauge corrected, whereas PERSIANN is a real-time product with no gauge-correction component.

For the purpose of evaluating PERSIANN-CDR's application in hydrological modeling, two phases of study were designed. In the first phase, the main goal was to test how PERSIANN-CDR's performance compares with the performance of other precipitation products. To have all the products available, the time period of 2003–10 was selected. The HL-RDHM was run

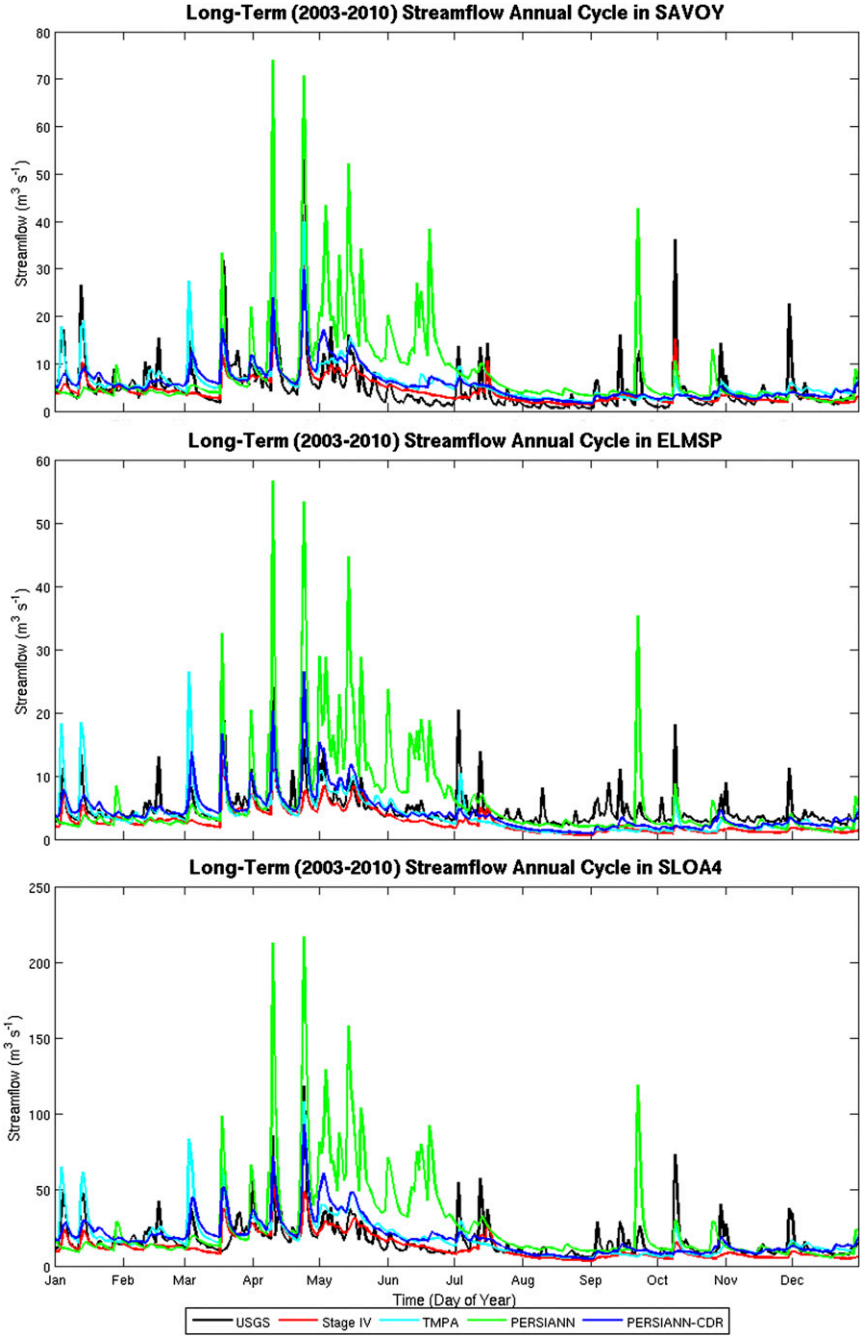

FIG. 8. Long-term (2003–10) annual cycle from USGS observation and stage IV–, TMPA-, PERSIANN-, and PERSIANN-CDR-derived hydrographs for (top) SAVOY, (middle) ELMSP, and (bottom) SLOA4 basins.

separately for each of these precipitation data products to simulate streamflow hydrographs at the outlets of three DMIP2 study basins where NWS a priori parameters are available. The simulations at SAVOY, ELMSP, and SLOA4 basins were compared with USGS observations. The results show that PERSIANN-CDR- and TMPA-derived simulations have close performances with higher correlation coefficients and better RMSEs for TMPA and lower biases for PERSIANN-CDR. Annual cycle analysis of simulated hydrographs also depicts close performance between TMPA and PERSIANN-CDR. Phase 1 of this study serves as

TABLE 3. As in Table 2, but for day-of-year long-term (2003–10) annual cycle analysis.

Product	Mean ($m^3 s^{-1}$)	Std dev ($m^3 s^{-1}$)	RMSE ($m^3 s^{-1}$)	CORR	ln E	BIAS	d
SAVOY							
PERSIANN	7.86	8.7	7.24	0.56	−0.388	62.7%	0.664
PERSIANN-CDR	5.56	3.39	4.16	0.673	0.313	15.2%	0.754
Stage IV	4.21	2.99	3.66	0.804	0.601	−12.7%	0.802
TMPA	5.88	4.24	3.6	0.767	0.330	21.78%	0.843
ELMSP							
PERSIANN	5.83	7.01	5.83	0.588	−1.325	26.61%	0.580
PERSIANN-CDR	4.14	3.03	2.38	0.666	−0.451	−10.09%	0.802
Stage IV	2.72	1.95	2.02	0.685	−2.541	−41.05%	0.694
TMPA	3.83	3.39	2.63	0.653	−1.074	−16.85%	0.776
SLOA4							
PERSIANN	26.13	28.23	23.76	0.557	−0.827	59.52%	0.560
PERSIANN-CDR	18.46	11.9	9.99	0.649	0.306	12.71%	0.792
Stage IV	12.47	8.16	8.96	0.660	0.118	−23.89%	0.749
TMPA	18.13	13.44	9.83	0.706	0.355	10.67%	0.826

the proof of concept regarding the applicability of PERSIANN-CDR in rainfall–runoff modeling. Given this result and the fact that PERSIANN-CDR precipitation data span from 1983 to the present, we could extend the simulation process back to 1983 to reconstruct the historical record of streamflow. This is particularly important when even USGS streamflow observations are not available prior to the year 1996 for the three study basins. In this phase of the study, only PERSIANN-CDR precipitation data were available as the forcing to the model. The resulting PERSIANN-CDR-derived hydrographs were compared with USGS observations depicting high CORR, relatively low BIAS, and high index of agreement criterion.

It is noteworthy that for the three DMIP2 study basins there were periods of time, mostly before 1996, when USGS daily data were not available. Using PERSIANN-CDR and HL-RDHM, we could simulate the streamflow for those periods and fill the gaps. This is particularly important for long-term trend studies where full data coverage over a long period of time, at least 30 years according to a World Meteorological Organization (WMO) report (Burroughs 2003), is needed. To conclude, PERSIANN-CDR could prove its usefulness

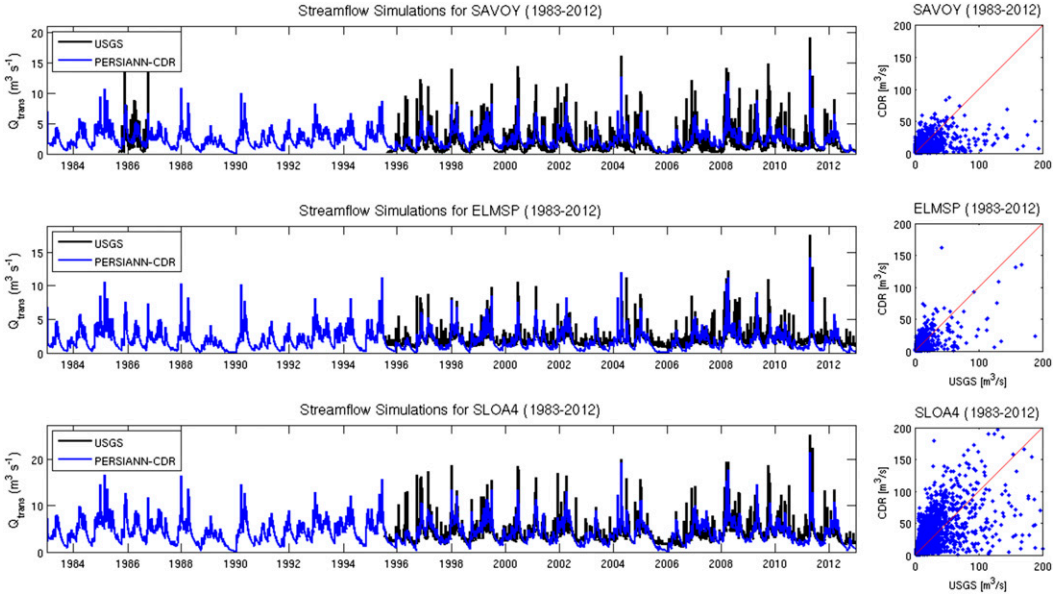

FIG. 9. Long-term (1983–2012) simulated streamflow from PERSIANN-CDR daily precipitation data (blue) vs USGS streamflow observations (black) for (top) SAVOY, (middle) ELMSP, and (bottom) SLOA4 basins, plus the respective scatterplots (right).

TABLE 4. BIAS, CORR, and RMSE statistics for simulated streamflow from PERSIANN-CDR against USGS observed streamflow for 1983–2012.

	Mean ($m^3 s^{-1}$)	Std dev ($m^3 s^{-1}$)	RMSE ($m^3 s^{-1}$)	CORR	ln E	BIAS	d
SAVOY	5.65	8.1	13.4	0.6719	0.265	12.24%	0.681
ELMSP	4.04	7.23	6.49	0.7342	−1.81	−10.9%	0.83
SLOA4	18.2	28.3	29.4	0.7344	0.236	5.26%	0.81

for long-term hydrological rainfall–runoff modeling and streamflow simulation. It can be particularly helpful for simulating streamflow in ungauged basins.

Acknowledgments. Partial financial support for this research was provided from the National Oceanic and Atmospheric Administration's (NOAA) Cooperative Institute for Climate and Satellites (CICS) and NOAA's National Centers for Environmental Information (NCEI) Climate Data Record program (Prime Award NA14NES4320003 and NCSU CICS Subaward 2014-2918-03), and fellowship programs from the NASA Earth and Space Science Fellowship (NESSF, NNX12AO11H) and Department of Defense (DoD) National Defense Science and Engineering Graduate Fellowship (NDSEG).

REFERENCES

Anagnostou, E. N., V. Maggioni, E. I. Nikolopoulos, T. Meskele, F. Hossain, and A. Papadopoulos, 2010: Benchmarking high-resolution global satellite rainfall products to radar and rain-gauge rainfall estimates. *IEEE Trans. Geosci. Remote Sens.*, **48**, 1667–1683, doi:10.1109/TGRS.2009.2034736.

Ashouri, H., K.-L. Hsu, S. Sorooshian, D. K. Braithwaite, K. R. Knapp, L. D. Cecil, B. R. Nelson, and O. P. Prat, 2015: PERSIANN-CDR: Daily precipitation climate data record from multisatellite observations for hydrological and climate studies. *Bull. Amer. Meteor. Soc.*, **96**, 69–83, doi:10.1175/BAMS-D-13-00068.1.

——, S. Sorooshian, K. Hsu, M. G. Bosilovich, J. Lee, and M. F. Wehner, 2016: Evaluation of NASA's MERRA precipitation product in reproducing the observed trend and distribution of extreme precipitation events in the United States. *J. Hydrometeor.*, **17**, 693–711, doi:10.1175/JHM-D-15-0097.1.

Bajracharya, S. R., W. Palash, M. S. Shrestha, V. R. Khadgi, C. Duo, P. J. Das, and C. Dorji, 2015: Systematic evaluation of satellite-based rainfall products over the Brahmaputra basin for hydrological applications. *Adv. Meteor.*, **2015**, 398687, doi:10.1155/2015/398687.

Behrangi, A., B. Khakbaz, T. C. Jaw, A. AghaKouchak, K. Hsu, and S. Sorooshian, 2011: Hydrologic evaluation of satellite precipitation products over a mid-size basin. *J. Hydrol.*, **397**, 225–237, doi:10.1016/j.jhydrol.2010.11.043.

Bergstrom, S., 1995: The HBV model. *Computer Models of Watershed Hydrology*, V. P. Singh, Ed., Water Resources Publications, 443–476.

Beven, K. J., 2011: *Rainfall–Runoff Modelling: The Primer*. Wiley, 488 pp.

Burnash, R. J. C., R. L. Ferral, and R. A. McGuire, 1973: A generalized streamflow simulation system: Conceptual modeling for digital computers. NWS/California Department of Water Resources Tech. Rep., 204 pp.

Burroughs, W., 2003: *Climate into the 21st Century*. Cambridge University Press, 240 pp.

Casse, C., and M. Gosset, 2015: Analysis of hydrological changes and flood increase in Niamey based on the PERSIANN-CDR satellite rainfall estimate and hydrological simulations over the 1983–2013 period. *Proc. IAHS*, **370**, 117–123, doi:10.5194/piahs-370-117-2015.

Ceccherini, G., I. Ameztoy, C. P. R. Hernández, and C. C. Moreno, 2015: High-resolution precipitation datasets in South America and West Africa based on satellite-derived rainfall, enhanced vegetation index and digital elevation model. *Remote Sens.*, **7**, 6454–6488, doi:10.3390/rs70506454.

Ciabatta, L., L. Brocca, C. Massari, T. Moramarco, S. Gabellani, S. Puca, and W. Wagner, 2016: Rainfall–runoff modelling by using SM2RAIN-derived and state-of-the-art satellite rainfall products over Italy. *Int. J. Appl. Earth Obs. Geoinf.*, **48**, 163–173, doi:10.1016/j.jag.2015.10.004.

Collischonn, B., W. Collischonn, and C. E. Morelli Tucci, 2008: Daily hydrological modeling in the Amazon basin using TRMM rainfall estimators. *J. Hydrol.*, **360**, 207–216, doi:10.1016/j.jhydrol.2008.07.032.

Ebert, E. E., J. E. Janowiak, and C. Kidd, 2007: Comparison of near-real-time precipitation estimates from satellite observations and numerical models. *Bull. Amer. Meteor. Soc.*, **88**, 47–64, doi:10.1175/BAMS-88-1-47.

Estupina-Borrell, V., D. Dartus, and R. Ababou, 2006: Flash flood modeling with the MARINE hydrological distributed model. *Hydrol. Earth System Sci. Discuss.*, **3**, 3397–3438, doi:10.5194/hessd-3-3397-2006.

Fulton, R. A., J. P. Breidenbach, D. J. Seo, D. A. Miller, and T. O'Bannon, 1998: The WSR-88D rainfall algorithm. *Wea. Forecasting*, **13**, 377–395, doi:10.1175/1520-0434(1998)013<0377:TWRA>2.0.CO;2.

Guetter, A. K., K. P. Georgakakos, and A. A. Tsonis, 1996: Hydrologic applications of satellite data: 2. Flow simulation and soil water estimates. *J. Geophys. Res.*, **101**, 26 527–26 538, doi:10.1029/96JD01655.

Guo, H., S. Chen, A. Bao, J. Hu, A. S. Gebregiorgis, X. Xue, and X. Zhang, 2015: Inter-comparison of high-resolution satellite precipitation products over central Asia. *Remote Sens.*, **7**, 7181–7211, doi:10.3390/rs70607181.

Hagos, S. M., L. R. Leung, J. H. Yoon, J. Lu, and Y. Gao, 2016: A projection of changes in landfalling atmospheric river frequency and extreme precipitation over western North America from the large ensemble CESM simulations. *Geophys. Res. Lett.*, **43**, 1357–1363, doi:10.1002/2015GL067392.

Harris, A., S. Rahman, F. Hossain, L. Yarborough, A. C. Bagtzoglou, and G. Easson, 2007: Satellite-based flood modeling using TRMM-based rainfall products. *Sensors*, **7**, 3416–3427, doi:10.3390/s7123416.

Hogue, T. S., S. Sorooshian, H. Gupta, A. Holz, and D. Braatz, 2000: A multistep automatic calibration scheme for river

forecasting models. *J. Hydrometeor.*, **1**, 524–542, doi:10.1175/1525-7541(2000)001<0524:AMACSF>2.0.CO;2.

Hong, Y., R. Adler, and G. Huffman, 2006: Evaluation of the potential of NASA multi-satellite precipitation analysis in global landslide hazard assessment. *Geophys. Res. Lett.*, **33**, L22402, doi:10.1029/2006GL028010.

Hsu, K., X. Gao, S. Sorooshian, and H. V. Gupta, 1997: Precipitation Estimation From Remotely Sensed Information Using Artificial Neural Networks. *J. Appl. Meteor. Climatol.*, **36**, 1176–1190, doi:10.1175/1520-0450(1997)036<1176:PEFRSI>2.0.CO;2.

——, H. V. Gupta, X. Gao, and S. Sorooshian, 1999: Estimation of physical variables from multichannel remotely sensed imagery using a neural network: Application to rainfall estimation. *Water Resour. Res.*, **35**, 1605–1618, doi:10.1029/1999WR900032.

Huffman, G. J., and D. T. Bolvin, 2013: GPCP version 2.2 SG combined precipitation data set documentation. NASA GSFC Doc., 46 pp. [Available online at ftp://precip.gsfc.nasa.gov/pub/gpcp-v2.2/doc/V2.2_doc.pdf.]

——, and Coauthors, 2007: The TRMM Multisatellite Precipitation Analysis (TMPA): Quasi-global, multiyear, combined-sensor precipitation estimates at fine scales. *J. Hydrometeor.*, **8**, 38–55, doi:10.1175/JHM560.1.

——, R. F. Adler, D. T. Bolvin, and E. J. Nelkin, 2010: The TRMM Multi-Satellite Precipitation Analysis (TMPA). *Satellite Rainfall Applications for Surface Hydrology*, M. Gebremichael and F. Hossain, Eds., Springer, 3–22, doi:10.1007/978-90-481-2915-7_1.

——, D. T. Bolvin, D. Braithwaite, K. Hsu, R. Joyce, C. Kidd, E. J. Nelkin, and P. Xie, 2015: NASA Global Precipitation Measurement Integrated Multi-satellitE Retrievals for GPM (IMERG). Algorithm Theoretical Basis Doc., version 4.5, 30 pp. [Available online at http://pmm.nasa.gov/sites/default/files/document_files/IMERG_ATBD_V4.5.pdf.]

Joyce, R. J., J. E. Janowiak, P. A. Arkin, and P. Xie, 2004: CMORPH: A method that produces global precipitation estimates from passive microwave and infrared data at high spatial and temporal resolution. *J. Hydrometeor.*, **5**, 487–503, doi:10.1175/1525-7541(2004)005<0487:CAMTPG>2.0.CO;2.

Khakbaz, B., B. Imam, K. Hsu, and S. Sorooshian, 2012: From lumped to distributed via semi-distributed: Calibration strategies for semi-distributed hydrologic models. *J. Hydrol.*, **418–419**, 61–77, doi:10.1016/j.jhydrol.2009.02.021.

Kim, G., and A. P. Barros, 2001: Quantitative flood forecasting using multisensor data and neural networks. *J. Hydrol.*, **246**, 45–62, doi:10.1016/S0022-1694(01)00353-5.

Knapp, K. R., 2008a: Scientific data stewardship of International Satellite Cloud Climatology Project B1 global geostationary observations. *J. Appl. Remote Sens.*, **2**, 023548, doi:10.1117/1.3043461.

——, 2008b: Calibration assessment of ISCCP geostationary infrared observations using HIRS. *J. Atmos. Oceanic Technol.*, **25**, 183–195, doi:10.1175/2007JTECHA910.1.

——, and Coauthors, 2011: Globally gridded satellite observations for climate studies. *Bull. Amer. Meteor. Soc.*, **92**, 893–907, doi:10.1175/2011BAMS3039.1.

Koren, V., and C. B. Barrett, 1994: Satellite based distributed monitoring, forecasting and simulation (MFS) system for the Nile River. *Proc. Int. Workshop on Application of Remote Sensing in Hydrology, NHRI Symp. 14*, Saskatoon, Canada, NHRI, 187–200.

——, M. Smith, and Q. Duan, 2003: Use of a priori parameter estimates in the derivation of spatially consistent parameter sets of rainfall–runoff models. *Calibration of Watershed Models*, Q. Duan et al., Eds., Water Science and Application Series, Vol. 6, Amer. Geophys. Union, 239–254.

——, S. Reed, M. Smith, Z. Zhang, and D.-J. Seo, 2004: Hydrology laboratory research modeling system (HL-RMS) of the US National Weather Service. *J. Hydrol.*, **291**, 297–318, doi:10.1016/j.jhydrol.2003.12.039.

——, M. Smith, Z. Cui, and B. Cosgrove, 2007: Physically-based modifications to the Sacramento Soil Moisture Accounting model: Modeling the effects of frozen ground on the rainfall–runoff process. NOAA Tech. Rep. NWS 52, 43 pp. [Available online at www.nws.noaa.gov/oh/hrl/hsmb/docs/hydrology/PBE_SAC-SMA/NOAA_Technical_Report_NWS_52.pdf.]

Kuzmin, V., D.-J. Seo, and V. Koren, 2008: Fast and efficient optimization of hydrologic model parameters using a priori estimates and stepwise line search. *J. Hydrol.*, **353**, 109–128, doi:10.1016/j.jhydrol.2008.02.001.

Legates, D. R., and G. J. McCabe Jr., 1999: Evaluating the use of "goodness-of-fit" measures in hydrologic and hydroclimatic model validation. *Water Resour. Res.*, **35**, 233–241, doi:10.1029/1998WR900018.

Liang, X., D. P. Lettenmaier, E. F. Wood, and S. J. Burges, 1994: A simple hydrologically based model of land surface water and energy fluxes for GSMs. *J. Geophys. Res.*, **99**, 14 415–14 428, doi:10.1029/94JD00483.

Luchetti, N. T., J. R. Sutton, E. E. Wright, M. C. Kruk, and J. J. Marra, 2016: When El Niño rages: How satellite data can help water-stressed islands. *Bull. Amer. Meteor. Soc.*, doi:10.1175/BAMS-D-15-00219.1, in press.

Maggioni, V., H. J. Vergara, E. N. Anagnostou, J. J. Gourley, Y. Hong, and D. Stampoulis, 2013: Investigating the applicability of error correction ensembles of satellite rainfall products in river flow simulations. *J. Hydrometeor.*, **14**, 1194–1211, doi:10.1175/JHM-D-12-074.1.

Miao, C., H. Ashouri, K.-L. Hsu, S. Sorooshian, and Q. Duan, 2015: Evaluation of the PERSIANN-CDR daily rainfall estimates in capturing the behavior of extreme precipitation events over China. *J. Hydrometeor.*, **16**, 1387–1396, doi:10.1175/JHM-D-14-0174.1.

Nash, J. E., and J. V. Sutcliffe, 1970: River flow forecasting through conceptual models. Part I—A discussion of principles. *J. Hydrol.*, **10**, 282–290, doi:10.1016/0022-1694(70)90255-6.

Nguyen, P., S. Sellars, A. Thorstensen, Y. Tao, H. Ashouri, D. Braithwaite, K. Hsu, and S. Sorooshian, 2014: Satellites track precipitation of Super Typhoon Haiyan. *Eos, Trans. Amer. Geophys. Union*, **95**, 133–135, doi:10.1002/2014EO160002.

——, A. Thorstensen, S. Sorooshian, K. Hsu, and A. AghaKouchak, 2015: Flood forecasting and inundation mapping using HiResFlood-UCI and near-real-time satellite precipitation data: The 2008 Iowa flood. *J. Hydrometeor.*, **16**, 1171–1183, doi:10.1175/JHM-D-14-0212.1.

——, and Coauthors, 2016: A high resolution coupled hydrologic–hydraulic model (HiResFlood-UCI) for flash flood modeling. *J. Hydrol.*, doi:10.1016/j.jhydrol.2015.10.047, in press.

NWS, 2011: Hydrology Laboratory-Research Distributed Hydrologic Model (HL-RDHM) user manual V. 3.2.0. National Weather Service Rep., 79 pp.

Piotrowski, A., J. J. Napiorkowski, and P. M. Rowinski, 2006: Flash-flood forecasting by means of neural networks and nearest neighbour approach—A comparative study. *Nonlinear Processes Geophys.*, **13**, 443–448, doi:10.5194/npg-13-443-2006.

Qi, W., C. Zhang, G. Fu, C. Sweetapple, and H. Zhou, 2016: Evaluation of global fine-resolution precipitation products and their uncertainty quantification in ensemble discharge simulations. *Hydrol. Earth Syst. Sci.*, **20**, 903–920, doi:10.5194/hess-20-903-2016.

Reed, S., J. Schaake, and Z. Zhang, 2007: A distributed hydrologic model and threshold frequency-based method for flash flood forecasting at ungauged locations. *J. Hydrol.*, **337**, 402–420, doi:10.1016/j.jhydrol.2007.02.015.

Rossow, W. B., and R. A. Schiffer, 1991: ISCCP cloud data products. *Bull. Amer. Meteor. Soc.*, **72**, 2–20, doi:10.1175/1520-0477(1991)072<0002:ICDP>2.0.CO;2.

——, and L. C. Garder, 1993: Cloud detection using satellite measurements of infrared and visible radiances for ISCCP. *J. Climate*, **6**, 2341–2369, doi:10.1175/1520-0442(1993)006<2341:CDUSMO>2.0.CO;2.

Sahoo, G. B., C. Ray, and E. H. De Carlo, 2006: Calibration and validation of a physically distributed hydrological model, MIKE SHE, to predict streamflow at high frequency in a flashy mountainous Hawaii stream. *J. Hydrol.*, **327**, 94–109, doi:10.1016/j.jhydrol.2005.11.012.

Schneider, U., T. Fuchs, A. Meyer-Christoffer, and B. Rudolf, 2008: Global precipitation analysis products of the GPCC. Global Precipitation Climatology Centre Doc., DWD, 14 pp. [Available online at ftp://ftp.dwd.de/pub/data/gpcc/PDF/GPCC_intro_products_2008.pdf.]

Seyyedi, H., E. N. Anagnostou, E. Beighley, and J. McCollum, 2015: Hydrologic evaluation of satellite and reanalysis precipitation datasets over a mid-latitude basin. *Atmos. Res.*, **164–165**, 37–48, doi:10.1016/j.atmosres.2015.03.019.

Sirdas, S., and Z. Sen, 2007: Determination of flash floods in western Arabian Peninsula. *J. Hydrol. Eng.*, **12**, 676–681, doi:10.1061/(ASCE)1084-0699(2007)12:6(676).

Smith, M. B., D.-J. Seo, V. I. Koren, S. M. Reed, Z. Zhang, Q. Duan, F. Moreda, and S. Cong, 2004: The distributed model intercomparison project (DMIP): Motivation and experiment design. *J. Hydrol.*, **298**, 4–26, doi:10.1016/j.jhydrol.2004.03.040.

——, and Coauthors, 2012a: The distributed model intercomparison project—Phase 2: Motivation and design of the Oklahoma experiments. *J. Hydrol.*, **418–419**, 3–16, doi:10.1016/j.jhydrol.2011.08.055.

——, and Coauthors, 2012b: Results of the DMIP 2 Oklahoma experiments. *J. Hydrol.*, **418–419**, 17–48, doi:10.1016/j.jhydrol.2011.08.056.

Solmon, F., V. S. Nair, and M. Mallet, 2015: Increasing Arabian dust activity and the Indian summer monsoon. *Atmos. Chem. Phys.*, **15**, 8051–8064, doi:10.5194/acp-15-8051-2015.

Sorooshian, S., K.-L. Hsu, X. Gao, H. V. Gupta, B. Imam, and D. Braithwaite, 2000: Evaluation of PERSIANN system satellite-based estimates of tropical rainfall. *Bull. Amer. Meteor. Soc.*, **81**, 2035–2046, doi:10.1175/1520-0477(2000)081<2035:EOPSSE>2.3.CO;2.

Stisen, S., and I. Sandholt, 2010: Evaluation of remote-sensing-based rainfall products through predictive capability in hydrological runoff modeling. *Hydrol. Processes*, **24**, 879–891, doi:10.1002/hyp.7529.

Su, F. G., Y. Hong, and D. P. Lettenmaier, 2008: Evaluation of TRMM Multisatellite Precipitation Analysis (TMPA) and its utility in hydrologic prediction in La Plata basin. *J. Hydrometeor.*, **9**, 622–640, doi:10.1175/2007JHM944.1.

Tang, Y., P. Reed, K. Van Werkhoven, and T. Wagener, 2007: Advancing the identification and evaluation of distributed rainfall–runoff models using global sensitivity analysis. *Water Resour. Res.*, **43**, W06415, doi:10.1029/2006WR005813.

Thiemig, V., R. Rojas, M. Zambrano-Bigiarini, and A. D. Roo, 2013: Hydrological evaluation of satellite-based rainfall estimates over the Volta and Baro–Akobo basin. *J. Hydrol.*, **499**, 324–338, doi:10.1016/j.jhydrol.2013.07.012.

Turk, J. T., G. V. Mostovoy, and V. Anantharaj, 2010: The NRL-Blend high resolution precipitation product and its application to land surface hydrology. *Satellite Rainfall Applications for Surface Hydrology*, M. Gebremichael and F. Hossain, Eds., Springer, 85–104, doi:10.1007/978-90-481-2915-7_6.

Wagener, T., K. van Werkhoven, P. Reed, and Y. Tang, 2009: Multiobjective sensitivity analysis to understand the information content in streamflow observations for distributed watershed modeling. *Water Resour. Res.*, **45**, W02501, doi:10.1029/2008WR007347.

Willmot, C. J., 1984: On the evaluation of model performance in physical geography. *Spatial Statistics and Models*, G. L. Gaile and C. J. Willmot, Eds., D. Reidel, 443–460.

Yang, X., B. Yong, H. Yong, S. Chen, and X. Zhang, 2016: Error analysis of multi-satellite precipitation estimates with an independent raingauge observation network over a medium-sized humid basin. *Hydrol. Sci. J.*, **61**, 1813–1830, doi:10.1080/02626667.2015.1040020.

Yilmaz, K. K., T. S. Hogue, K. L. Hsu, S. Sorooshian, H. V. Gupta, and T. Wagener, 2005: Intercomparison of rain gauge, radar, and satellite-based precipitation estimates with emphasis on hydrologic forecasting. *J. Hydrometeor.*, **6**, 497–517, doi:10.1175/JHM431.1.

——, H. V. Gupta, and T. Wagener, 2008: A process-based diagnostic approach to model evaluation: Application to the NWS distributed hydrologic model. *Water Resour. Res.*, **44**, W09417, doi:10.1029/2007WR006716.

Yong, B., 2015: Comments on ''Error analysis of satellite precipitation products in mountainous basins.'' *J. Hydrometeor.*, **16**, 1443–1444, doi:10.1175/JHM-D-14-0202.1.

Zeweldi, D. A., and M. Gebremichael, 2009: Evaluation of CMORPH precipitation products at fine space–time scales. *J. Hydrometeor.*, **10**, 300–307, doi:10.1175/2008JHM1041.1.